I/O System Performance Debugging
Using Model-driven Anomaly Characterization[*]

Kai Shen   Ming Zhong   Chuanpeng Li
Department of Computer Science, University of Rochester
{kshen, zhong, cli}@cs.rochester.edu

Abstract

It is challenging to identify performance problems and pinpoint their root causes in complex systems, especially when the system supports wide ranges of workloads and when performance problems only materialize under particular workload conditions. This paper proposes a model-driven anomaly characterization approach and uses it to discover operating system performance bugs when supporting disk I/O-intensive online servers. We construct a whole-system I/O throughput model as the reference of expected performance and we use statistical clustering and characterization of performance anomalies to guide debugging. Unlike previous performance debugging methods offering detailed statistics at specific execution settings, our approach focuses on comprehensive anomaly characterization over wide ranges of workload conditions and system configurations.

Our approach helps us quickly identify four performance bugs in the I/O system of the recent Linux 2.6.10 kernel (one in the file system prefetching, two in the anticipatory I/O scheduler, and one in the elevator I/O scheduler). Our experiments with two Web server benchmarks, a trace-driven index searching server, and the TPC-C database benchmark show that the corrected kernel improves system throughput by up to five-fold compared with the original kernel (averaging 6%, 32%, 39%, and 16% for the four server workloads).

1 Introduction

It is not uncommon for complex systems to perform worse than expected. In the context of this paper, we define performance bugs as problems in system implementation that degrade the performance (compared with that intended by the design protocol/algorithm). Examples of such bugs include overly-simplified implementations, mis-management of special cases, or plain erroneous coding. These bugs, upon discovery, are typically quite easy to fix in comparison with implementing newer and better protocol/algorithms. However, it is challeng-

ing to identify performance problems and pinpoint their root causes in large software systems.

Previous techniques such as program instrumentation [13, 20], complete system simulation [24], performance assertion checking [22], and detailed overhead categorization [9] were proposed to understand performance problems in complex computer systems and applications. Some recent performance debugging work employs statistical analysis of online system traces [1, 7] to identify faulty components in large systems. In general, these techniques focus on offering fine-grained examination of the target system/application in specific execution settings. However, many systems (such as the I/O system in OS) are designed to support wide ranges of workload conditions and they may also be configured in various different ways. It is desirable to explore performance anomalies over a comprehensive universe of execution settings for these systems. Such exploration is particularly useful for performance debugging without the knowledge of runtime workload conditions and system configurations.

We propose a new approach that systematically characterizes performance anomalies in a system to aid performance debugging. The key advantage is that we can comprehensively consider wide ranges of workload conditions and system configurations. Our approach proceeds in the following steps (shown in Figure 1).

1. We construct a whole-system performance model according to the design protocol/algorithms of relevant system components. The model predicts system performance under different workload conditions and system configurations.

2. We acquire a representative set of anomalous workload and system configuration settings by comparing measured system performance with model prediction under a number of sample settings. For each system component that is considered for debugging, we include some sample settings where the component is bypassed.

3. We statistically cluster anomalous settings into groups likely attributed to individual "causes". We then characterize each such cause (or bug) with correlated system component and workload conditions.
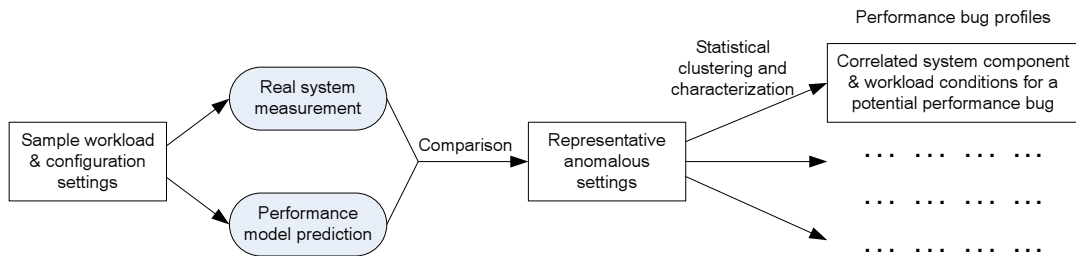
Figure 1: High-level overview of the proposed model-driven anomaly characterization.

The result of our approach contains profiles for potential performance bugs, each with a system component where the bug is likely located and the settings (workload conditions and system configurations) where it would inflict significant performance losses. Such result then assists further human debugging. It also helps verifying or explaining bugs after they are discovered. Even if some bugs could not be immediately fixed, our anomaly characterization identifies workload conditions and system configurations that should be avoided if possible.

Note that discrepancies between measured system performance and model prediction can also be caused by errors in the performance model. Therefore, we must examine both the performance model and the system implementation when presented with a bug profile. Since the performance model is much less complex in nature, we focus on debugging the system implementation in this paper.

It is possible for our approach to have false positives (producing characterizations that do not correspond to any real bugs) and false negatives (missing some bugs in the output). As a debugging aid where human screening is available, false positives are less of a concern. In order to achieve low false negatives, we sample wide ranges of workload parameters and various system configurations in a systematic fashion.

The rest of this paper presents our approach in details and describes our experience of discovering operating system performance bugs when supporting disk I/O-intensive online servers. Although our results in this paper focus on one target system and one type of workloads, we believe that the proposed model-driven anomaly characterization approach is general. It may assist the performance debugging of other systems and workloads as long as comprehensive performance models can be built for them.

2 Background

2.1 Targeted Workloads

The targeted workloads in this work are data-intensive online servers that access large disk-resident datasets while serving multiple clients simultaneously. Examples include Web servers hosting large datasets and keyword search engines that support interactive search on terabytes of indexed Web pages. In these servers, each incoming request is serviced by a request handler which can be a thread in a multi-threaded server or a series of event handlers in an event-driven server. The request handler repeatedly accesses disk data and consumes CPU before completion. A request handler may block if the needed resource is unavailable. While request handlers consume both disk I/O and CPU resources, the overall server throughput is often dominated by I/O system performance when application data size far exceeds available server memory. For the ease of model construction in the next section, we assume that request handlers perform mostly read-only I/O when accessing disk-resident data. Many online services, such as Web server and index searching, do not involve any updates on hosted datasets.

Characteristics of the application workload may affect the performance of a disk I/O-intensive online server. For example, the data access locality and sequentiality largely determine how much of the disk time is spent on data transfer or seek and rotation.

2.2 Relevant Operating System Components

We describe operating system features that affect the I/O performance of data-intensive online servers.

Prefetching. Data accesses belonging to a single request handler often exhibit strong locality due to semantic proximity. During concurrent execution, however, data access of one request handler can be frequently interrupted by other active request handlers in the server. This may severely affect I/O efficiency due to long disk seek and rotational delays. The employment of OS prefetching can partially alleviate this problem. A larger prefetching depth increases the granularity of I/O requests, and consequently yields less frequent disk seeks and rotations. On the other hand, kernel-level prefetching may retrieve unneeded data due to the lack of knowledge on how much data is desired by the application. Such a waste tends to be magnified by aggressive prefetching policies.

I/O scheduling. Traditional elevator-style I/O schedulers such as Cyclic-SCAN sort and merge outstanding I/O requests to reduce the seek distance on storage devices. In addition, the anticipatory I/O scheduling [14] can be particularly effective for concurrent I/O workloads. At the completion of an I/O request, the anticipatory disk scheduler may choose to keep the disk idle for a short period of time even when there are pending requests. The scheduler does so in anticipation of a new I/O request from the same process that issued the just completed request, which often requires little or no seeking from the current disk head location. However, anticipatory scheduling may not be effective when substantial think time exists between consecutive I/O requests. The anticipation may also be rendered ineffective when a request handler has to perform interleaving synchronous I/O that does not exhibit strong locality. Such a situation arises when a request handler simultaneously accesses multiple data streams.

Others. For data-intensive workloads, memory caching is effective in improving the application-perceived performance over the raw storage I/O throughput. Most operating systems employ LRU-style policies to manage data cached in memory.

File system implementation issues such as file layout can also affect the system performance. We assume the file data is laid out contiguously on the storage. This is a reasonable assumption since the OS often tries to allocate file data contiguously on creation and the dataset is unchanged under our targeted read-only workloads.

3 I/O Throughput Model

Our model-driven performance debugging requires model-based prediction of the overall system performance under wide ranges of workload conditions and various system configurations. Previous studies have recognized the importance of constructing I/O system performance models. Various analytical and simulation models have been constructed for disk drives [5, 16, 25, 28, 36], disk arrays [8, 33], OS prefetching [6, 29, 31], and memory caching [15]. However, performance models for individual system components do not capture the inter-dependence of different components and consequently they may not accurately predict the overall application performance.

When modeling a complex system like ours, we follow the methodology of decomposing it into weakly coupled subcomponents. More specifically, we divide our whole-system I/O throughput model into four layers — OS caching, prefetching, OS-level I/O scheduling, and the storage device. Every layer may transform its input workload to a new workload imposed on the lower layer. For example, I/O scheduling may alter inter-request I/O
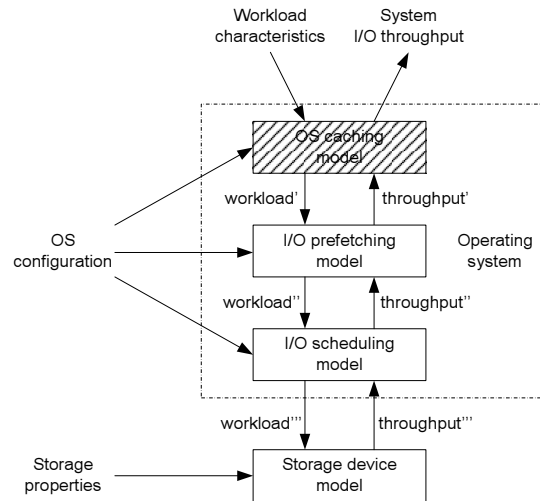

Figure 2: Layered system model on I/O throughput. We bypass the OS caching model in the context of this paper.

seek distances. Each layer may also change the predicted I/O throughput from the lower layer due to additional benefits or costs it may induce. For instance, prefetching adds the potential overhead of fetching unneeded data. As indicated in Figure 2, we use $workload$, $workload'$, $workload''$, and $workload'''$ to denote the original and transformed workloads at each layer. We similarly use $throughput$, $throughput'$, $throughput''$, and $throughput'''$ to represent the I/O throughput results seen at each layer.

Figure 2 illustrates our layered system model on I/O throughput. This paper focuses on the I/O system performance debugging and we bypass the OS caching model in our study. For the purpose of comparing our performance model with real system measurement, we add additional code in the operating system to disable the caching. More information on this is provided in Section 4.1. The rest of this section illustrates the other three layers of the I/O throughput model in detail. While mostly applicable to many general-purpose OSes, our model more closely follows the target system of our debugging work — the Linux 2.6 kernel.

3.1 OS Prefetching Model

We define a *sequential access stream* as a group of spatially contiguous data items that are accessed by a single request handler. Note that the request handler may not continuously access the entire stream at once. In other words, it may perform interleaving I/O that does not belong to the same stream. We further define a *sequential access run* as a portion of a sequential access stream that does not have such interleaving I/O. Figure 3 illustrates these two concepts. All read accesses from request handlers are assumed to be synchronous.
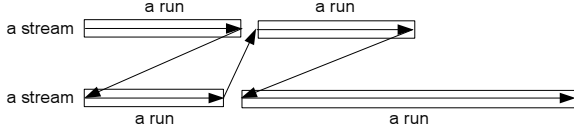
Figure 3: Illustration of the sequential access stream and the sequential access run. The arrows indicate the data access sequence of the request handler.

We consider the workload transformation of I/O prefetching on a sequential access stream of length S_{stream}. I/O prefetching groups data accesses of the stream into requests of size $S_{prefetch}$ — the I/O prefetching depth. Therefore, the number of I/O requests for serving this sequential stream is:

$$N_{request} = \lceil \frac{S_{stream}}{S_{prefetch}} \rceil \qquad (1)$$

Operating system prefetching may retrieve unneeded data due to the lack of knowledge on how much data is desired by the application. In the transformed workload, the total amount of fetched data for the stream is:

$$S'_{stream} = \lceil \frac{S_{stream}}{S_{prefetch}} \rceil \cdot S_{prefetch} \qquad (2)$$

Within the amount of fetched data S'_{stream}, the effective amount is only S_{stream} while the rest is not needed by the application. Therefore:

$$throughput' = throughput'' \cdot \frac{\sum S_{stream}}{\sum S'_{stream}} \qquad (3)$$

However, wasted prefetching does not exist when each sequential access stream references a whole file since the OS would not prefetch beyond the end of a file. In this case, I/O prefetching does not fetch unneeded data and it does not change the I/O throughput. Therefore:

$$S'_{stream} = S_{stream} \qquad (4)$$

$$throughput' = throughput'' \qquad (5)$$

3.2 OS-level I/O Scheduling Model

The I/O scheduling layer passes the retrieved data to the upper layer without any change. Therefore it does not change the I/O throughput:

$$throughput'' = throughput''' \qquad (6)$$

I/O scheduling transforms the workload primarily by sorting and merging I/O requests to reduce the seek distance on storage devices. We discuss such workload transformation by the traditional elevator-style I/O scheduling and by the anticipatory I/O scheduling.

3.2.1 Elevator-style I/O Scheduling

I/O scheduling algorithms such as Cyclic-SCAN reorder outstanding I/O requests based on data location and schedule the I/O request close to the current disk head location. The effectiveness of such scheduling is affected by the concurrency of the online server. Specifically, a smaller average seek distance can be attained at higher server concurrency when the disk scheduler can choose from more concurrent requests for seek reduction. We estimate that the number of simultaneous disk seek requests in the SCAN queue is equal to the server concurrency level γ. When the disk scheduler can choose from γ requests at uniformly random disk locations, a previous study [27] indicates that the inter-request seek distance D_{seek} follows the following distribution:

$$Pr[D_{seek} \geq x] = (1 - \frac{x}{\delta \cdot D_{disk}})^{\gamma} \qquad (7)$$

Here δ is the proportion of the disk where the dataset resides and D_{disk} is the total disk size. In other words, $\delta \cdot D_{disk}$ represents the span of the dataset on the disk.

During concurrent execution (concurrency greater than one), the I/O scheduler switches to a different stream when a prefetching request from one stream is completed. Therefore it does not change the granularity of I/O requests passed from the prefetching layer. Consequently the average size of an I/O request is:

$$E(S_{request}) = \frac{\sum S'_{stream}}{\sum N_{request}} = \frac{E(S'_{stream})}{E(N_{request})} \qquad (8)$$

At the concurrency of one, all I/O requests belonging to one sequential access run is merged:

$$E(S_{request}) = \max\{\frac{E(S'_{stream})}{E(N_{request})}, E(S_{run})\} \qquad (9)$$

where $E(S_{run})$ is the average length of a sequential access run.

3.2.2 Anticipatory I/O Scheduling

During concurrent execution, the anticipatory I/O scheduling [14] may temporarily idle the disk so that consecutive I/O requests that belong to the same request handler are serviced without interruption. This effectively merges all prefetching requests of each sequential access run (defined in Section 3.1) into a single I/O request. Thus the average size of an I/O request in the transformed workload is:

$$E(S_{request}) = \max\{\frac{E(S'_{stream})}{E(N_{request})}, E(S_{run})\} \qquad (10)$$

The anticipatory I/O scheduling likely reduces the frequency of disk seeks, but it does not affect the the inter-request seek distance modeled in Equation (7).

The other effect of the anticipatory I/O scheduling is that it induces disk idle time during anticipatory waiting when useful work could be otherwise performed. The disk idle time for each I/O request T_{idle} is the total inter-request thinktime for the corresponding sequential access run.

3.3 Storage Device Model

Let the disk transfer rate be R_{tr}. Also let the seek time and rotational delay be T_{seek} and $T_{rotation}$ respectively. The disk resource consumption (in time) for processing a request of length $S_{request}$ includes a single seek, rotation, and the data transfer as well as the idle time:

$$\mathcal{T}_{disk} = \frac{S_{request}}{R_{tr}} + T_{seek} + T_{rotation} + T_{idle} \quad (11)$$

Since $S_{request}$ is independent of R_{tr}, we have:

$$E(\mathcal{T}_{disk}) = \frac{E(S_{request})}{E(R_{tr})} + E(T_{seek}) + E(T_{rotation}) + E(T_{idle}) \quad (12)$$

Therefore:

$$\begin{aligned}
&throughput''' \\
&= \frac{E(S_{request})}{E(\mathcal{T}_{disk})} \\
&= \frac{E(S_{request})}{\frac{E(S_{request})}{E(R_{tr})} + E(T_{seek}) + E(T_{rotation}) + E(T_{idle})}
\end{aligned} \quad (13)$$

Below we determine the average data transfer rate $E(R_{tr})$, the average rotation delay $E(T_{rotation})$, and the average seek time $E(T_{seek})$. The sequential transfer rate depends on the data location (due to zoning on modern disks). With the knowledge of the data span on the disk and the histogram of data transfer rate at each disk location, we can then determine the average data transfer rate. We consider the average rotational delay as the mean rotational time between two random track locations (*i.e.*, the time it takes the disk to spin half a revolution).

Earlier studies [25, 28] have discovered that the seek time depends on the seek distance D_{seek} (distance to be traveled by the disk head) in the following way:

$$T_{seek} = \begin{cases} 0, & \text{if } D_{seek} = 0; \\ a + b\sqrt{\frac{D_{seek}}{D_{disk}}}, & \text{if } 0 < \frac{D_{seek}}{D_{disk}} \le e; \\ c + d \cdot \frac{D_{seek}}{D_{disk}}, & \text{if } e < \frac{D_{seek}}{D_{disk}} \le 1. \end{cases} \quad (14)$$

where D_{disk} is the total disk size. a, b, c, d, e are disk-specific parameters and $a + b\sqrt{e} \approx c + d \cdot e$.

Combining the seek distance distribution in Equation (7) and the above Equation (14), we have the following cumulative probability distribution for the seek time:

$$Pr[T_{seek} \ge x] = \begin{cases} 1, & \text{if } x \le a; \\ \left(1 - \frac{(\frac{x-a}{b})^2}{\delta}\right)^{\gamma}, & \text{if } a < x \le a + b\sqrt{e}; \\ \left(1 - \frac{(\frac{x-c}{d})}{\delta}\right)^{\gamma}, & \text{if } c + d \cdot e < x \le c + d \cdot \delta; \\ 0, & \text{if } c + d \cdot \delta < x. \end{cases} \quad (15)$$

Therefore, the expected average seek time is:

$$\begin{aligned}
&E(T_{seek}) \\
&= \int_0^a Pr[T_{seek} \ge x]dx + \int_a^{a+b\cdot\sqrt{e}} Pr[T_{seek} \ge x]dx \\
&\quad + \int_{c+d\cdot e}^{c+d\cdot\delta} Pr[T_{seek} \ge x]dx \\
&= a + \int_a^{a+b\sqrt{e}} \left(1 - \frac{(\frac{x-a}{b})^2}{\delta}\right)^{\gamma} dx + \int_{c+d\cdot e}^{c+d\cdot\delta} \left(1 - \frac{(\frac{x-c}{d})}{\delta}\right)^{\gamma} dx \\
&= a + b \cdot \int_0^{\sqrt{e}} \left(1 - \frac{x^2}{\delta}\right)^{\gamma} dx + d \cdot \int_e^{\delta} \left(1 - \frac{x}{\delta}\right)^{\gamma} dx \\
&= a + b\sqrt{e} \cdot \left(\sum_{i=0}^{\gamma} \frac{\binom{\gamma}{i}}{2i+1} \cdot (-\frac{e}{\delta})^i\right) + \frac{d \cdot \delta}{\gamma + 1} \cdot (1 - \frac{e}{\delta})^{\gamma+1}
\end{aligned}$$

where $\binom{\gamma}{i}$ indicates the binomial coefficient.

$$(16)$$

Disk drives are usually equipped with limited amount of cache. Due to its small size, its main usage is disk track prefetching while its caching effects are negligible for data-intensive applications with large working-set sizes. We do not consider such caching effects in our model.

3.4 Symbol Definitions

For clarity, we list the definitions for all symbols used in the previous subsections (Table 1).

3.5 Model Interfaces

We summarize the interfaces to our performance model, which include the workload characteristics, operating system configuration, and storage device properties.

- Table 2 lists the attributes of workload characteristics passed into our model. The table also lists the OS component in our performance model that is most concerned with each workload attribute.
- The OS configuration consists of the I/O prefetching depth and whether to employ the anticipatory I/O scheduler or the classic elevator scheduler.
- The storage device properties include the disk size, rotational speed, seek time model parameters of Equation (14), and the histogram of data transfer rate at each disk location.

Symbol	Definition
S_{stream}, S'_{stream}	original and transformed sequential access stream lengths
S_{run}	the sequential access run length
$S_{prefetch}$	I/O prefetching depth
$N_{prefetch}$	the number of I/O prefetching requests for accessing a stream
$S_{request}$	the I/O request size
γ	the number of concurrent request executions in the server
D_{seek}, D_{disk}	the seek distance and the total disk size
δ	the proportion of the dataset span to the total disk size
$T_{seek}, T_{rotation}, T_{idle}, \mathcal{T}_{disk}$	the disk seek, rotation, idle, and total usage time
R_{tr}	the disk data transfer rate
a, b, c, d, e	disk-specific parameters concerning the disk seek time

Table 1: Definition of symbols used in Section 3.

Workload attribute	Unit	Concerned OS component
server concurrency	a number	I/O scheduling (Section 3.2)
data span on storage medium	ratio to the disk size	I/O scheduling (Section 3.2)
lengths of sequential access streams	a histogram	I/O prefetching (Section 3.1)
whether each stream access whole file	true or false	I/O prefetching (Section 3.1)
average sequential access run length	unit of data size	anticipatory I/O scheduling (Section 3.2.2)
average application thinktime	unit of time	anticipatory I/O scheduling (Section 3.2.2)

Table 2: Attributes of workload characteristics. We also list the OS component in our performance model that is most concerned with each workload attribute.

4 Model-driven Performance Debugging

Based on the whole-system performance model for I/O-intensive online servers, this section describes our approach to acquire a representative set of anomalous workload and configuration settings. We also present techniques to cluster anomalous settings into groups likely attributed to individual bugs. We then characterize each of them with correlated system component and workload conditions. Although certain low-level techniques in our approach are specifically designed for our target system and workloads, we believe the general framework of our approach can also be used for performance debugging of other large software systems.

4.1 Anomaly Sampling

Performance anomalies (manifested by deviations of measurement results from the model-predicted performance) occur for several reasons. In addition to performance bugs in the implementation, measurement errors and model inaccuracies can also cause performance anomalies. Aside from significant modeling errors, anomalies caused by these other factors are usually small in magnitude. We screen out these factors by only counting the relatively large performance anomalies. Although this screening may also overlook some performance bugs, those that cause significant performance degradations would not be affected.

Performance anomalies may occur at many different workload conditions and system configurations. We con-

sider each occurrence under one setting as a single point in the multi-dimensional space where each workload condition and system configuration parameter is represented by a dimension. For the rest of this paper, we call this multi-dimensional space simply as the *parameter space*. Our anomaly sampling proceeds in the following two steps. First, we choose a number of (n) sample settings from the parameter space in a uniformly random fashion. We then compare measured system performance with model prediction under these settings. Anomalous settings are those at which measured performance trails model prediction by at least a certain threshold.

We define the *infliction zone* of each performance bug as the union of settings in the parameter space at which the bug would inflict significant performance losses. By examining a uniformly random set of sample settings, our anomaly sampling approach can achieve the following property associated with false negatives (missing some bugs). For a bug whose infliction zone is p proportion ($0 < p \leq 1$) of the total parameter space, the probability for at least one of our n random samples falls into the bug's infliction zone is $1 - (1 - p)^n$. With a reasonably large n, it is unlikely for our anomaly sampling to miss a performance bug that takes effects under a non-trivial set of workload conditions and system configurations.

We now describe the parameter space for our target workload and system. We first explore the dimensions representing workload properties and we will examine the system configuration dimensions next.

Workload properties The inclusion of each workload property in the parameter space allows the characterization of its relationship with performance bugs in subsequent analysis. However, considering too many workload properties may render the subsequent analysis intractable. According to our performance model in Section 3, we select workload properties from those that have large effects on system performance. For each workload property, we determine several representative parameter settings for possible sampling.

- *Server concurrency*: 1, 2, 4, 8, 16, 32, 64, 128, 256.
- *Average length of sequential access streams*: 64 KB, 128 KB, 256 KB, 512 KB, 1 MB, 2 MB, 4 MB.
- *Whether each stream access whole file*: true or false.
- *Average length of sequential access runs*: 16 KB, 32 KB, 64 KB, $\cdots$, up to the average length of sequential access streams.
- *Average application thinktime per megabyte of data access*: 1 ms, 2 ms, 4 ms, 8 ms.

For the purpose of real system measurement, we design an adjustable micro-benchmark that can exhibit any combination of workload parameter settings.

System configurations The inclusion of system configurations in the parameter space allows the characterization of their relationships with performance bugs in subsequent analysis. In particular, the strong correlation between a performance bug and the activation of a system component indicates the likelihood that the bug is within the implementation of the said component. As indicated in our performance model, the system performance is mainly affected by three I/O system components: prefetching, the elevator I/O scheduler and the anticipatory I/O scheduler.

For each system component that is considered for debugging, we must include system configurations where the component is not activated. The two I/O schedulers are natural alternatives to each other. We augment the operating system to add an option to bypass the prefetching code. We do so by ignoring the readahead heuristics and issuing I/O requests only when data is synchronously demanded by the application. Since our performance model does not consider OS caching, we also add additional code in the operating system to disable the caching. We do so by simply overlooking the cached pages during I/O. Our changes are only a few hundred lines in the Linux 2.6.10 kernel.

Below are the specific dimensions in our parameter space that represent system configurations:

- *Prefetching*: enabled or disabled.
- *I/O scheduling*: elevator or anticipatory.

Our performance model in Section 3 can predict system performance at different prefetching sizes. However, varying the prefetching size is not useful for our purpose of performance debugging. We use the default maximum prefetching size (128 KB for Linux 2.6.10) in our study.

4.2 Anomaly Clustering and Characterization

Given a set of anomalous workload condition and system configuration settings, it is still hard to derive useful debugging information without a succinct characterization on the anomalous settings. Further, the system may contain multiple independent performance bugs and the aggregate characteristics of several bugs may be too confusing to be useful. This section presents an algorithm to cluster anomalous settings into groups likely attributed to individual bugs and characterize each cluster to guide performance debugging. At a high level, the anomaly sampling described in Section 4.1 precedes the clustering and characterization, which are then followed by the final human debugging. Ideally, each such action sequence can discover one performance bug and multiple bugs can be identified by iterating this action sequence multiple times.

It is quite common for infliction zones of multiple bugs to cross-intersect with each other. In other words, several bugs might inflict performance losses simultaneously at a single workload condition and system configuration. Classical clustering algorithms such as Expectation Maximization (EM) [10] and K-means [19] typically assume disjoint (or slightly overlapped) clusters and spherical Gaussian distribution for points in each cluster. Therefore they cannot be directly used to solve our problem.

To make our clustering problem more tractable, we assume that the infliction zone of each performance bug takes a hyper-rectangle-like shape in the parameter space. This means that if parameter settings $(a_1, a_2, ..., a_k)$ and $(b_1, b_2, ..., b_k)$ in the k-dimensional parameter space are inflicted by a bug, then any parameter setting $(x_1, x_2, ..., x_k)$ with

$$\begin{cases} a_1 \leq x_1 \leq b_1 \\ a_2 \leq x_2 \leq b_2 \\ \cdots\cdots \\ a_k \leq x_k \leq b_k \end{cases} \quad (17)$$

also likely falls into the bug's infliction zone. For each dimension i that has no ordering among its value settings (*e.g.*, a boolean or categorical parameter), the corresponding element in Condition (17) should be instead "$x_i = a_i$ or $x_i = b_i$".

A bug's infliction zone takes a hyper-rectangle-like shape if it has a range of triggering settings on each parameter (workload property or system configuration)

and the bug's performance effect is strongly correlated with the condition that all parameters fall into respective triggering ranges. When this assumption does not hold for a bug (*i.e.*, its infliction zone does not follow a hyper-rectangle-like shape), our algorithm described below would identify a maximum hyper-rectangle encapsulated within the bug's infliction zone. This might still provide some useful bug characterization for subsequent human debugging.

To the best of our knowledge, the only known clustering algorithm that handles intersected hyper-rectangles is due to Pelleg and Moore [21]. However, their algorithm requires hyper-rectangles to have *soft* boundaries with Gaussian distributions and hence is not directly applicable to our case, where hyper-rectangles could have infinitely steeply diminishing borders.

We describe our algorithm that identifies and characterizes one dominant cluster from a set of anomalous settings. More specifically, our algorithm attempts to identify a hyper-rectangle in the parameter space that explores trade-off between two properties: 1) Most of the sample settings within the hyper-rectangle are anomalous settings; 2) The hyper-rectangle contains as many anomalous settings as possible. In our algorithm, property 1 is ensured by keeping the ratio of $\frac{\# \ of \ anomalies}{\# \ of \ samples}$ in the hyper-rectangle above a certain pre-defined threshold. Property 2 is addressed by greedily expanding the current hyper-rectangle in a way to maximize the number of anomalous settings contained in the expanded new hyper-rectangle. Algorithm 4.1 illustrates our method to discover a hyper-rectangle that tightly bounds the cluster of anomalous settings related to a dominant bug.

After the hyper-rectangle clustering, we characterize each cluster by simply projecting the hyper-rectangle onto each dimension of the parameter space. For each dimension (a workload property or a system configuration), we include the projected parameter value range into the characterization. For those dimensions at which the projections cover all possible parameter values, we consider them uncorrelated to the cluster and we do not include them in the cluster characterization.

The computation complexity of our algorithm is $O(m^3 n)$ since the algorithm has three nested loops with at most m iterations for each. In the innermost loop, the numbers of samples and anomalies within a hyper-rectangle are computed by brute-force checking of all n sample settings (an $O(n)$ complexity). Using pre-constructed orthogonal range trees [18], the complexity of the innermost loop can be improved to $O((\log n)^d + A)$, where d is the dimensionality of the parameter space and A is the answer size. We use brute-force counting in our current implementation due to its simplicity and satisfactory performance on our dataset (no more than 1000 sample settings and less than 200 anomalies).

Algorithm 4.1: CLUSTER(n samples, m anomalies, ϵ)

Input: n sample settings.
Input: m anomalous settings among the samples.
Input: $0 < \epsilon \leq 1$, the threshold for $r(H)$.
Returns: H_{max}, a hyper-rectangle in the parameter space.

$H_{max} \leftarrow nil$

for each x out of m anomalous settings

do $\begin{cases} H \leftarrow \text{the min-bounding hyper-rectangle for } x \\ \\ \textbf{while } H \text{ was just expanded} \\ \textbf{do} \begin{cases} y_{tmp} \leftarrow nil \\ c_{tmp} \leftarrow 0 \\ \\ \textbf{for each} \text{ anomalous setting } y \text{ outside } H \\ \textbf{do} \begin{cases} \textbf{if } [r(M(H,y)) \geq \epsilon \\ \textbf{and } c(M(H,y)) > c_{tmp}] \\ \textbf{then } \begin{cases} y_{tmp} \leftarrow y \\ c_{tmp} \leftarrow c(M(H,y)) \end{cases} \end{cases} \\ \\ \textbf{if } [y_{tmp} \neq nil] \\ \quad \textbf{then } H \leftarrow M(H, y_{tmp}) \\ \\ \textbf{if } [c(H) > c(H_{max})] \\ \quad \textbf{then } H_{max} \leftarrow H \end{cases} \end{cases}$

return (H_{max})

/* $r(H)$ *denotes the ratio of* $\frac{\# \ of \ anomalies}{\# \ of \ samples}$ *in the hyper-rectangle* H.
$c(H)$ *denotes the number of anomalies in* H.
$M(H, y)$ *denotes the minimum-bounding hyper-rectangle that contains the hyper-rectangle* H *and the point* y. */

---

5 Debugging Results

We describe our performance debugging of the Linux 2.6.10 kernel (released in December 2004) when supporting I/O-intensive online servers. We repeatedly perform anomaly sampling, clustering, characterization, and human debugging. After each round, we acquire an anomaly cluster characterization that corresponds to one likely bug. The characterization typically contains correlated system component and workload conditions, which hints at where and how to look for the bug. The human debugger has knowledge on the general structure of the OS source code and is familiar with a kernel tracing tool (LTT [37]). After each bug fix, we use the corrected kernel for the next round of anomaly sampling, clustering, characterization, and human debugging.
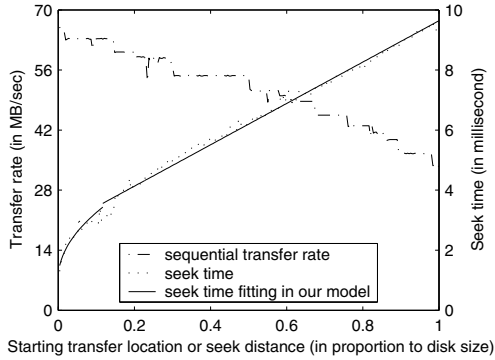
Figure 4: Data transfer rate and seek time curve for the disk drive. We also show the seek time fitting used in Equation (14) of our performance model.

Our measurement uses a server equipped with dual 2.0 GHz Xeon processors, 2 GB memory, and an IBM 10 KRPM SCSI drive (model "DTN036C1UCDY10"). We measure the disk drive properties as input to our performance model (shown in Figure 4). The Equation (14) parameters for this disk is a=1.0546 ms, b=6.9555 ms, c=2.7539 ms, d=6.8867 ms, and e=0.1171. We choose 400 random workload and system configuration settings in the anomaly sampling. The anomaly threshold is set at 10% (*i.e.*, those settings at which measured performance trails model prediction by at least 10% are considered as anomalous settings). The clustering threshold (ϵ) in Algorithm 4.1 is set at 90%.

We describe our results below and we also report the debugging time at the end of this section. The first anomaly cluster characterization is:

Workload property	
Concurrency:	128 and above
Stream length:	256KB and above
System configuration	
Prefetching:	enabled

This characterization shows that the corresponding bug concerns the prefetching implementation and it inflicts performance losses for high concurrency workloads with moderately long sequential access streams. Based on this information, our subsequent tracing and analysis discover the following performance bug. The kernel checks for disk congestion when each I/O prefetching is initiated. If the number of pending requests in the disk driver queue exceeds a certain threshold (slightly below 128 in Linux 2.6.10), the prefetching is canceled. The intuition for this treatment is that asynchronous read-*ahead* should be disabled when the I/O system is busy. However, the prefetching operations may include some data that is synchronously demanded by the application. By canceling these operations, it causes confusion at upper-level I/O code and results in inefficient single-page makeup I/Os

for the needed data. In order to fix this problem, the corrected kernel only cancels prefetching requests that do not contain any synchronously demanded data when disk congestion occurs. We call this *bug fix #1*.

The second anomaly cluster characterization is:

Workload property	
Concurrency:	8 and above
Stream length:	256KB and above
Run length:	256KB and above
System configuration	
I/O scheduling:	anticipatory

This characterization concerns the anticipatory I/O scheduler. It involves workloads at moderately high concurrency with stream and run lengths larger than the maximum prefetching size (128 KB). Our subsequent investigation discovers the following performance bug. The current implementation of the anticipatory scheduler stops an ongoing anticipation if there exists a pending I/O request with shorter seek distance (compared with the average seek distance of the anticipating process). Due to a significant seek initiation cost on modern disks (as shown in Figure 4), the seek distance is not an accurate indication of the seek time cost. For example, the average cost of a 0-distance seek and a $2x$-distance seek is much less than an x-distance seek. As the result, the current implementation tends to stop the anticipation when the benefit of continued anticipation actually exceeds that of breaking it. We solve this problem by using estimated seek time (instead of the seek distance) in the anticipation cost/benefit analysis. We call this *bug fix #2*.

The third anomaly cluster characterization is:

Workload property	
Concurrency:	2
System configuration	
I/O scheduling:	elevator

This characterization concerns the elevator scheduler (also called the deadline scheduler in Linux 2.6.10) and the corresponding bug inflicts performance losses at the concurrency of 2. Our tracing and analysis show that a `reset` function is called frequently at very low concurrency. Possibly due to an overly-simplified implementation, the kernel always searches from block address 0 for the next scheduled request after the reset. We fix it by searching from the last I/O location according to the elevator scheduling algorithm. We call this *bug fix #3*.

The fourth anomaly cluster characterization is:

Workload property	
Concurrency:	2 and above
Stream length:	256KB and above
Run length:	256KB
System configuration	
I/O scheduling:	anticipatory

This characterization concerns the anticipatory I/O scheduler for non-serial concurrent workloads. Our subsequent investigation uncovers the following problem. Large I/O requests (including maximum-sized prefetching requests) from the file system are often split into smaller pieces before being forwarded to the disk drive. The completion of each one of these pieces will trigger an I/O interrupt. The original anticipatory scheduler would start the anticipation timer right after the first such interrupt, which often causes premature timeout. We correct the problem by starting the anticipation timer only after all pieces of a file system I/O request have completed. We call this *bug fix #4*.

We show results on the effects of our bug fixes. Figure 5 shows the top 10% model/measurement errors of our anomaly sampling for the original Linux 2.6.10 kernel and after the accumulative bug fixes. The error is defined as "$1 - \frac{\text{measured throughput}}{\text{model-predicted throughput}}$". Results show that performance anomalies steadily decrease after each bug fix and no anomaly with 14% or larger error exists after all four bugs are fixed. Figure 6 illustrates all-sample comparison between model prediction and measured performance. Figure 6(A) shows results for the original Linux 2.6.10 where the system performs significantly worse than model prediction at many parameter settings. Figure 6(B) shows the results when all four bugs are fixed where the system performs close to model prediction at all parameter settings.

Debugging time We provide statistics on the debugging time. For each bug fix, time is spent on anomaly sampling, clustering and characterization, and final human debugging.

- The primary time cost for anomaly sampling is on the system measurement for all sample workload condition and system configuration settings. The measurement of each sample setting took around 6 minutes and the total 400 sample measurements took around two days using one test server. More test servers would speed up this process proportionally.

- Due to the relative small sample size, our clustering and characterization algorithm took less than a minute to complete.

- The final human debugging took about one or two days for each bug fix.

6   Evaluation with Real Workloads

We experiment with real server workloads to demonstrate the performance benefits of our bug fixes. All measurements are conducted on servers each equipped with
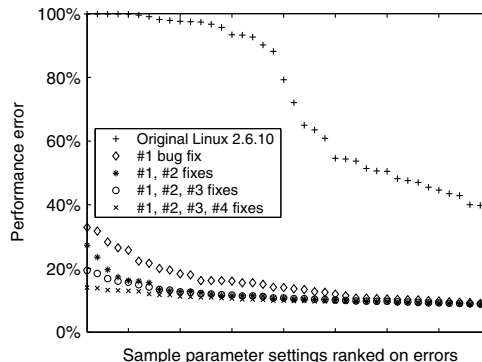

Figure 5: Top 10% model/measurement errors. Each unit on the X-axis represents a sampled parameter setting in our anomaly sampling.

dual 2.0 GHz Xeon processors, 2 GB memory, and an IBM 10 KRPM SCSI drive (as characterized in Figure 4). Each experiment involves a server and a load generation client. The client can adjust the number of simultaneous requests to control the server concurrency level.

6.1   Workload Descriptions

We evaluate four server workloads in our study:

- *SPECweb99:* We include the SPECweb99 benchmark [30] running on the Apache 2.0.44 Web server. This workload contains 4 classes of files with sizes at 1 KB, 10 KB, 100 KB, and 1,000 KB respectively. During each run, the four classes of files are accessed according to a distribution that favors small files. Within each class, a Zipf distribution with parameter $\alpha = 1.0$ is used to access individual files.

- *Media clips:* Web workloads such as SPECweb99 contain mostly small file accesses. In order to examine the effects of relatively large sequential access streams, we use a Web workload containing a set of media clips, following the file size and access distribution of the video/audio clips portion of the 1998 World Cup workload [3]. About 67% (in total size) of files in the workload are large video clips, while the rest are small audio clips. The file sizes of both small and large clips follow Lognormal distributions, with average sizes of 20 KB and 1,464 KB respectively. During the tests, individual media files are chosen as client requests in a uniformly random fashion.

- *Index searching:* We acquired a prototype of the index searching server and a dataset from the Web search engine Ask Jeeves [4]. The dataset contains the search index for 12.6 million Web pages. It includes a mapping file that maps MD5-encoded keywords to proper locations in the search index. For
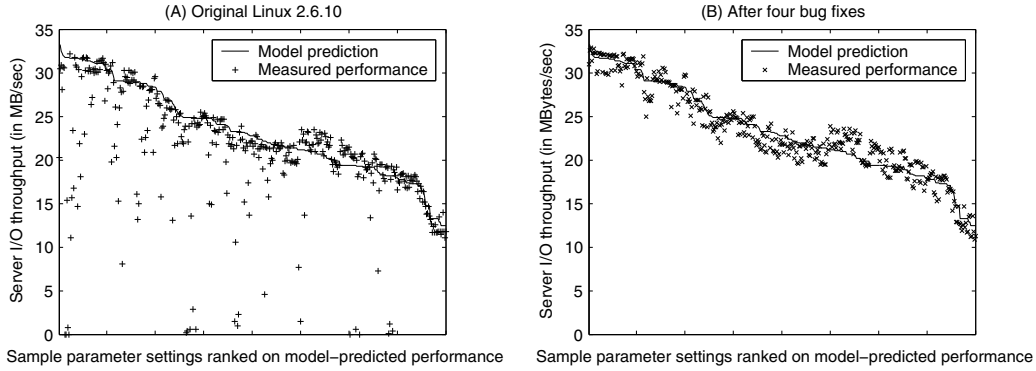
Figure 6: All-sample comparison between model prediction and measured performance. Each unit on the X-axis represents a sampled parameter setting in our anomaly sampling.

Workload	Data size	Data popularity	Whole file access	Mean stream len.	Runs/stream	Thinktime/MB
SPECweb99	22.4 GB	Zipf	yes	67.2 KB	1.00	1.11 ms
Media clips	27.2 GB	Uniformly random	yes	1213.3 KB	1.01	1.78 ms
Index searching	18.5 GB	Trace-driven	no	267.2 KB	1.75	0.22 ms
TPC-C	8.8 GB	Uniformly random	no	43.8 KB	1.00	11.69 ms

Table 3: Characteristics of four server workloads used in our evaluation.

each keyword in an input query, a binary search is first performed on the mapping file and then the search index is accessed following a sequential access pattern. Multiple prefetching streams on the search index are accessed for each multi-keyword query. The search query words in our test workload are based on a one-week trace recorded at the Ask Jeeves site in early 2002.

- *TPC-C database benchmark:* We include a local implementation of the TPC-C online transaction processing benchmark [32] in our evaluation. TPC-C simulates a population of terminal operators executing Order-Entry transactions against a database. Some of the TPC-C transactions do not consume much I/O resource. We use a workload that contains only the "new order" transactions, which are the most I/O-intensive among five types of TPC-C transactions. In our experiments, the TPC-C benchmark runs on the MySQL 5.0.2-alpha database with a dataset of 8.8 GB.

To better understand these workloads, we extract their characteristics through profiling. During profiling runs, we intercept relevant I/O system calls in the OS kernel, including `open`, `close`, `read`, `write`, and `seek`. We extract desired application characteristics after analyzing the system call traces collected during profiling runs. However, system call interception does not work well for memory mapped I/O used by the TPC-C database. In this case, we intercept device driver-level I/O traces and use them to infer the data access pattern of the workload. Table 3 lists some characteristics of the four server

workloads. The stream statistics for TPC-C are for read streams only. Among the four workloads, we observe that media clips has long sequential access streams while SPECweb99 and TPC-C have relatively short streams. We also observe that the three workloads except the index searching have about one run per stream, which indicates that each request handler does not perform interleaving I/O when accessing a sequential stream.

6.2 Performance Results

Figure 7 illustrates the throughput of the four server workloads. For each workload, we show measured performance at different concurrency levels under the original Linux kernel and after various performance bug fixes. The elevator I/O scheduler is employed for SPECweb99 and media clips while the anticipatory I/O scheduler is used for index searching and TPC-C. Therefore bug fix #3 is only meaningful for SPECweb99 and media clips while fixes #2 and #4 are only useful for index searching and TPC-C. The I/O throughput results are those observed at the application level. They are acquired by instrumenting the server applications with statistics-collection code. We were not able to make such instrumentation for the MySQL database used by TPC-C so we only show the request throughput for this workload.

Suggested by the characterization of bug #1, Figure 7(B) and (C) confirm substantial performance improvement (around five-fold) of the bug fix at high execution concurrencies. We notice that its effect is not as obvious for SPECweb99 and TPC-C. This can also be explained by our characterization of bug #1 since these
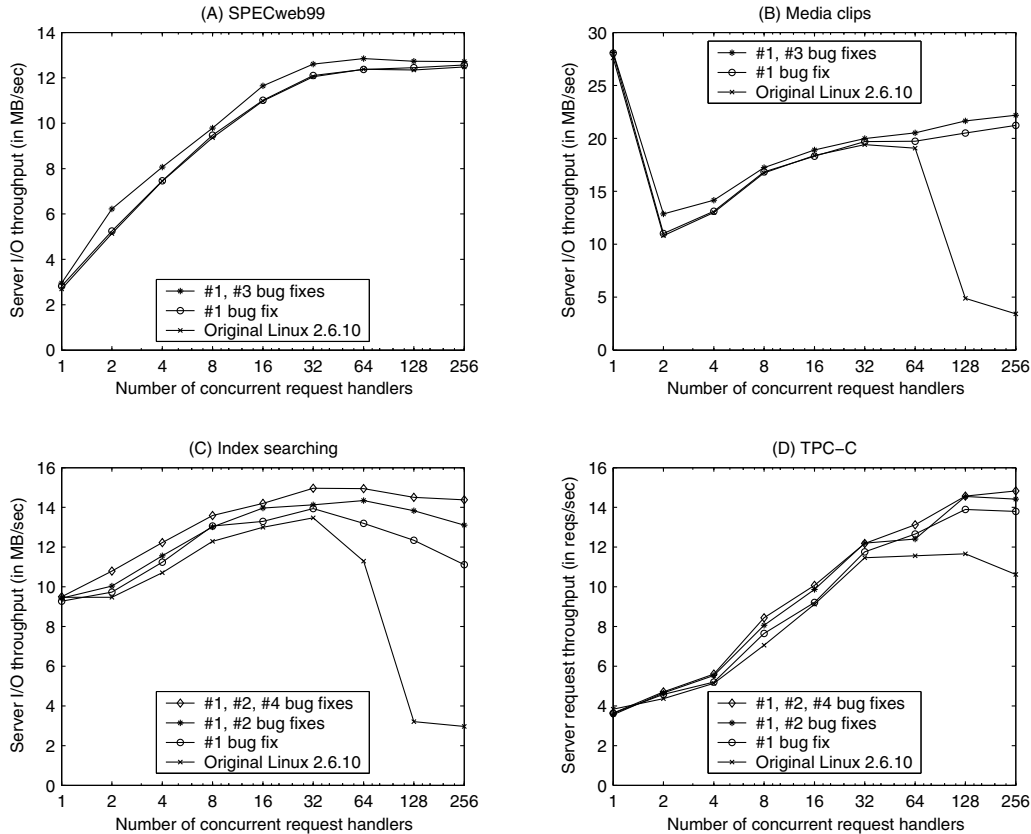
Figure 7: Throughput of four server workloads under various kernels. The elevator I/O scheduler is employed for SPECweb99 and media clips while the anticipatory I/O scheduler is used for index searching and TPC-C.

workloads do not have long enough sequential access streams. The other bug fixes provide moderate performance enhancement for workloads that they affect. The average improvement (over all affected workload conditions) is 6%, 13%, and 4% for bug fix #2, #3, and #4 respectively.

Aggregating the effects of all bug fixes, the average improvement (over all tested concurrencies) of the corrected kernel over the original kernel is 6%, 32%, 39%, and 16% for the four server workloads respectively.

7 Related Work

Performance debugging. Earlier studies have proposed techniques such as program instrumentation (*e.g.*, MemSpy [20] and Mtool [13]), complete system simulation (*e.g.*, SimOS [24]), performance assertion checking [22], and detailed overhead categorization [9] to understand performance problems in computer systems and applications. These techniques focus on offering fine-grained examination of the target system/application in specific workload settings. Many of them are too expensive to be used for exploring wide ranges of workload conditions and system configurations. In compari-

son, our approach trades off detailed execution statistics at specific settings for comprehensive characterization of performance anomalies over wide ranges of workloads.

Recent performance debugging work employs statistical analysis of online system traces [1, 7] to identify faulty components in complex systems. Such techniques are limited to reacting to anomalies under past and present operational environments and they cannot be used to debug a system before such operational conditions are known. Further, our approach can provide the additional information of correlated workload conditions with each potential performance bug, which is helpful to the debugging process.

Identifying non-performance bugs in complex systems. Several recent works investigated techniques to discover non-performance bugs in large software systems. Engler *et al.* detect potential bugs by identifying anomalous code that deviates from the common pattern [11]. Wang *et al.* discover erroneous system configuration settings by matching with a set of known correct configurations [34]. Li *et al.* employ data mining techniques to identify copy-paste and related bugs in operating system code [17]. However, performance-oriented debugging can be more challenging because many performance bugs are strongly connected with the code se-

mantics and they often do not follow certain patterns. Further, performance bugs may not cause obvious misbehaviors such as incorrect states or system crashes. Without an understanding on the expected performance (*e.g.*, through the performance model that we built), it may not even be easy to tell the existence of performance anomalies in complex systems.

I/O system performance modeling. Our performance debugging approach requires the construction of a whole-system performance model for targeted I/O-intensive server workloads. A large body of previous studies have constructed various analytical and simulation models to examine the performance of storage and I/O systems, including those for disk drives [5, 16, 25, 28, 36], disk arrays [2, 8, 33], I/O scheduling algorithms [23, 26, 35], and I/O prefetching [6, 29, 31]. However, performance models for individual system components do not capture the interplay between different components. This paper presents a whole-system throughput model that considers the combined impact of the application characteristics and several relevant operating system components on the overall server performance.

Using system-level models to predict the performance of I/O-intensive workloads is not new. Ganger and Patt argued that the I/O subsystem model must consider the *criticality* of I/O requests, which is determined by application and OS behaviors [12]. Shriver *et al.* studied I/O system performance using a combined disk and OS prefetching model [29]. However, these models do not consider recently proposed I/O system features. In particular, we are not aware of any prior I/O system modeling work that considers the anticipatory I/O scheduling, which can significantly affect the performance of our targeted workloads.

8   Conclusion

This paper presents a new performance debugging approach for complex software systems using model-driven anomaly characterization. In our approach, we first construct a whole-system performance model according to the design protocol/algorithms of the target system. We then acquire a representative set of anomalous workload settings by comparing measured system performance with model prediction under a number of sample settings. We statistically cluster the anomalous settings into groups likely attributed to individual bugs and characterize them with specific system components and workload conditions. Compared with previous performance debugging techniques, the key advantage of our approach is that we can comprehensively characterize performance anomalies of a complex system under wide ranges of workload conditions and system configurations.

We employ our approach to quickly identify four performance bugs in the I/O system of the recent Linux 2.6.10 kernel. Our anomaly characterization provides hints on the likely system component each performance bug may be located at and workload conditions for the bug to inflict significant performance losses. Experimental results demonstrate substantial performance benefits of our bug fixes on four real server workloads.

References

[1] M. K. Aguilera, J. C. Mogul, J. L. Wiener, P. Reynolds, and A. Muthitacharoen. Performance Debugging for Distributed Systems of Black Boxes. In *Proc. of the 19th ACM SOSP*, pages 74–89, Bolton Landing, NY, October 2003.

[2] E. Anderson, R. Swaminathan, A. Veitch, G. A. Alvarez, and J. Wilkes. Selecting RAID Levels for Disk Arrays. In *Proc. of the 1st USENIX Conf. on File and Storage Technologies*, pages 189–201, Monterey, CA, January 2002.

[3] M. Arlitt and T. Jin. Workload Characterization of the 1998 World Cup Web Site. Technical Report HPL-1999-35, HP Laboratories Palo Alto, 1999.

[4] Ask Jeeves Search. http://www.ask.com.

[5] R. Barve, E. Shriver, P. B. Gibbons, B. K. Hillyer, Y. Matias, and J. S. Vitter. Modeling and Optimizing I/O Throughput of Multiple Disks on A Bus. In *Proc. of the ACM SIGMETRICS*, pages 83–92, Atlanta, GA, June 1999.

[6] P. Cao, E. W. Felten, A. R. Karlin, and K. Li. A Study of Integrated Prefetching and Caching Strategies. In *Proc. of the ACM SIGMETRICS*, pages 188–197, Ottawa, Canada, June 1995.

[7] M. Chen, E. Kiciman, E. Fratkin, A. Fox, and E. Brewer. Pinpoint: Problem Determination in Large, Dynamic Systems. In *Proc. of Int'l Conf. on Dependable Systems and Networks*, pages 595–604, Washington, DC, June 2002.

[8] P. M. Chen, G. A. Gibson, R. H. Katz, and D. A. Patterson. An Evaluation of Redundant Arrays of Disks using an Amdahl 5890. In *Proc. of the ACM SIGMETRICS*, pages 74–85, Boulder, CO, May 1990.

[9] M. E. Crovella and T. J. LeBlanc. Parallel Performance Prediction Using Lost Cycles Analysis. In *Proc. of Super-Computing*, pages 600–610, Washington, DC, November 1994.

[10] A. P. Dempster, N. M. Laird, and D. B. Rubin. Maximum Likelihood from Incomplete Data Via the EM Algorithm. *Journal of the Royal Statistical Society, Series B*, (1):1–38, 1977.

[11] D. Engler, D. Chen, S. Hallem, A. Chou, and B. Chelf. Bugs as Deviant Behavior: A General Approach to Inferring Errors in Systems Code. In *Proc. of the 18th ACM SOSP*, pages 57–72, Banff, Canada, October 2001.

[12] G. R. Ganger and Y. N. Patt. Using System-Level Models to Evaluate I/O Subsystem Designs. *IEEE Trans. on Computers*, 47(6):667–678, June 1998.

[13] A. J. Goldberg and J. L. Hennessy. Mtool: An Integrated System for Performance Debugging Shared Memory Multiprocessor Applications. *IEEE Trans. on Parallel and Distributed Systems*, 4(1):28–40, January 1993.

[14] S. Iyer and P. Druschel. Anticipatory Scheduling: A Disk Scheduling Framework to Overcome Deceptive Idleness in Synchronous I/O. In *Proc. of the 18th ACM SOSP*, pages 117–130, Banff, Canada, October 2001.

[15] P. Jelenkovic and A. Radovanovic. The Persistent-Access-Caching Algorithm. Technical Report EE-2004-03-05, Dept. of Electrical Engineering, Columbia University, 2004.

[16] D. Kotz, S. B. Toh, and S. Radhakrishnan. A Detailed Simulation Model of the HP 97560 Disk Drive. Technical Report PCS-TR94-220, Dept. of Computer Science, Dartmouth College, July 1994.

[17] Z. Li, S. Lu, S. Myagmar, and Y. Zhou. CP-Miner: A Tool for Finding Copy-paste and Related Bugs in Operating System Code. In *Proc. of the 6th USENIX OSDI*, pages 289–302, San Francisco, CA, December 2004.

[18] G. S. Lueker. A Data Structure for Orthogonal Range Queries. In *Proc. of the 19th IEEE Symp. on Foundations of Computer Science*, pages 28–34, 1978.

[19] J. B. MacQueen. Some Methods for Classification and Analysis of Multivariate Observations. In *Proc. of the 5th Berkeley Symp. on Mathematical Statistics and Probability*, pages 281–297, 1967.

[20] M. Martonosi, A. Gupta, and T. Anderson. MemSpy: Analyzing Memory System Bottlenecks in Programs. In *Proc. of the ACM SIGMETRICS*, pages 1–12, Newport, RI, June 1992.

[21] D. Pelleg and A. Moore. Mixtures of Rectangles: Interpretable Soft Clustering. In *Proc. of the 18th Int'l Conf. on Machine Learning*, pages 401–408, Berkshires, MA, June 2001.

[22] S. E. Perl and W. E. Weihl. Performance Assertion Checking. In *Proc. of the 14th ACM SOSP*, pages 134–145, Asheville, NC, December 1993.

[23] F. I. Popovici, A. C. Arpaci-Dusseau, and R. H. Arpaci-Dusseau. Robust, Portable I/O Scheduling with the Disk Mimic. In *Proc. of the USENIX Annual Technical Conf.*, pages 297–310, San Antonio, TX, June 2003.

[24] M. Rosenblum, E. Bugnion, S. Devine, and S. A. Herrod. Using the SimOS Machine Simulator to Study Complex Computer Systems. *ACM Trans. on Modeling and Computer Simulation*, 7(1):78–103, January 1997.

[25] C. Ruemmler and J. Wilkes. An Introduction to Disk Drive Modeling. *IEEE Computer*, 27(3):17–28, March 1994.

[26] P. J. Shenoy and H. M. Vin. Cello: A Disk Scheduling Framework for Next Generation Operating Systems. In *Proc. of the ACM SIGMETRICS*, pages 44–55, Madison, WI, June 1998.

[27] E. Shriver. *Performance Modeling for Realistic Storage Devices*. PhD thesis, Dept of Computer Science, New York University, 1997.

[28] E. Shriver, A. Merchant, and J. Wilkes. An Analytical Behavior Model for Disk Drives with Readahead Caches and Request Reordering. In *Proc. of the ACM SIGMETRICS*, pages 182–192, Madison, WI, June 1998.

[29] E. Shriver, C. Small, and K. A. Smith. Why Does File System Prefetching Work? In *Proc. of the USENIX Annual Technical Conf.*, pages 71–84, Monterey, CA, June 1999.

[30] SPECweb99 Benchmark. http://www.specbench.org/osg/web99.

[31] A. Tomkins, R. H. Patterson, and G. A. Gibson. Informed Multi-Process Prefetching and Caching. In *Proc. of the ACM SIGMETRICS*, pages 100–114, Seattle, WA, June 1997.

[32] Transaction Processing Performance Council. TPC Benchmark C, Revision 5.4, April 2005. http://www.tpc.org/tpcc/.

[33] M. Uysal, G. A. Alvarez, and A. Merchant. A Modular, Analytical Throughput Model for Modern Disk Arrays. In *Proc. of the 9th MASCOTS*, pages 183–192, Cincinnati, OH, August 2001.

[34] H. J. Wang, J. C. Platt, Y. Chen, R. Zhang, and Y.-M. Wang. Automatic Misconfiguration Troubleshooting with PeerPressure. In *Proc. of the 6th USENIX OSDI*, pages 245–258, San Francisco, CA, December 2004.

[35] B. L. Worthington, G. R. Ganger, and Y. N. Patt. Scheduling Algorithms for Modern Disk Drives. In *Proc. of the ACM SIGMETRICS*, pages 241–251, Santa Clara, CA, May 1994.

[36] B. L. Worthington, G. R. Ganger, Y. N. Patt, and J. Wilkes. On-Line Extraction of SCSI Disk Drive Parameters. In *Proc. of the ACM SIGMETRICS*, pages 146–156, Ottawa, Canada, June 1995.

[37] K. Yaghmour and M. R. Dagenais. Measuring and Characterizing System Behavior Using Kernel-Level Event Logging. In *Proc. of the USENIX Annual Technical Conf.*, San Diego, CA, June 2000.